Solid State Phenomena
ISSN: 1662-9779, Vol. 362, pp 65-70
doi:10.4028/p-z8fjMB

Submitted: 2023-09-29
Revised: 2024-04-09
Accepted: 2024-04-12
Online: 2024-08-27

Influence of the Size Distribution of the SiC Powder Source on the Shape of the Crystal Growth Interface during PVT Growth of 4H-SiC Boules

J. Schultheiß[1,a], J. Ihle[1,b], S. Usseglio Nanot[2,c], S. Bonanomi[2,d], D. Callejo Munoz[2,e], R. Hammer[3,f], P. Wellmann[1,g,*]

[1]Crystal Growth Lab, Materials Department 6, Univ. of Erlangen-Nürnberg, Germany

[2]SiCreate GmbH, Via Piave 6, 23871 Lomagna (LC), Italy

[3]EEMCO GmbH, Ebner-Platz 1, 4060 Leonding, Austria

[a]jana.schultheiss@fau.de, [b]jonas.ihle@fau.de, [c]uns@sicreate.cc, [d]bon@sicreate.cc, [e]cal@sicreate.cc, [f]hamm@eemco.at, [g]peter.wellmann@fau.de

Keywords: SiC PVT growth, SiC source material, temperature field, mass transport

Abstract. We compared the evolution of three different SiC sources during standard PVT growth runs. The evolution of the growing crystal and the morphological changes in the SiC source were visualized using in-situ X-ray visualization. Computer simulation was used to calculate the temperature field distributions. It is found that the densification and shrinkage of the SiC source material during the growth process can affect the growth conditions in such a way that the convexity of the growth interface is increased in an unfavorable manner. While unfavorable growth conditions can be related to thermal properties due to less favorable SiC powder evolution, predicting such behavior is a rather complex task that still relies on the support of experimental methods.

Introduction

SiC crystals for commercial applications are mainly grown by the Physical Vapor Transport (PVT) process also known as seeded sublimation method. Typically, a source of SiC powder is heated to over 2000°C, while the seed placed above the source is slightly cooler (for a recent review see [1]). In many hot zone configurations, the property of the SiC source material affects the SiC growth interface. Depending on the SiC particle shape and size distribution, the SiC source material undergoes significant morphological changes during the growth process. A high packing density tends to cause less morphological changes [2]. Depending on the effective thermal conductivity of the SiC source, the isotherms at the crystal growth interface and between the SiC source and the SiC crystal may change. The latter can cause a change in the radial temperature gradient, which should be small. In addition, the axial temperature gradient can change, which affects the supersaturation in front of the growth interface and also affects the shape of the grown crystal [3]. All these phenomena limit the yield to grow SiC crystals with low dislocation density.

In this study we have investigated the influence the SiC source material on the PVT growth process with the aim to evaluate the run-to-run process stability. For this purpose, three SiC sources were selected, two of which were prepared by the same synthesis route, but different size distribution and particle shapes.

Experiments

The three SiC sources used in this study have the following characteristics: Source A consists of polycrystalline SiC chunks with a size of several millimeters. Source B and C have a particle size range of 0.1 - 1 mm and 0.1 - 2 mm, respectively. Table 1 provides a set of properties for the three SiC sources. In addition, data from a SiC powder source produced at FAU with an average particle diameter of about 0.2 mm have been added for comparison.

All growth runs were performed in an inductively heated PVT system using 100 mm 4H-SiC (4° off-axis) seeds. The growth process was monitored using 2D X-ray in-situ visualization [4] to detect

the morphological changes of the SiC source and the shape of the crystal growth interface. The heating power varied between 10.25 and 11 kW. The growth interface temperature and axial temperature gradients were determined by computer simulation.

Table 1. Properties of the SiC source materials.

Number	Type	Size	Initial packing density [g/cm^3]	Related porosity
Source A	Flakes	Several mm	1.31	41%
Source B	Powder	0.1 – 1 mm	1.44	45%
Source C	Powder	0.1 – 2 mm	1.50	47%
FAU ref.	Powder	0.2 mm	1.60	50%

Computer Simulation

Computer simulation of the temperature field was performed using the COMSOL Multi-Physics software package. The main challenge in calculating an accurate temperature field distribution is to provide an adequate material database of the carbon materials (dense graphite and various insulations) above 2000°C. For most of the hot zone components used in this study, the temperature dependent thermal conductivities were determined using laser flash measurements up to 1200°C and further extrapolation above 2000°C. In an iterative fitting routine, experimental and calculated temperature data were compared for different crucible heating process settings and bulk growth runs to determine precise high temperature material properties (see e.g. [5, 6]). The morphological changes within the SiC source material (= densified SiC feedstock and surrounding fluffy residual carbon skeleton) were accounted for by a two-region model using experimental in-situ X-ray visualization data as geometric input. Mass transport between the SiC source and growing crystal was performed following the work of [7-9]: Sublimation and crystallization at the source and seed was calculated following the Hertz-Knudsen approach. The growth rate limiting species is SiC_2. Side wall reaction with the graphite crucible were neglected. To account for the spatial extension of the subliming porous SiC powder material, a molar mass flux from a volumetric source was implemented into the model.

Results and Discussion

Packing Density. Often, SiC sources with higher packing densities exhibit a smothering sublimation-recrystallization behavior, while source materials with low packing densities undergo greater morphological changes.

Fig. 1 shows the crystal growth interface at approximately the midpoint of the growth process. Fig. 2 shows the crystal growth interface and the final morphological property of the starting material of each SiC powder type.

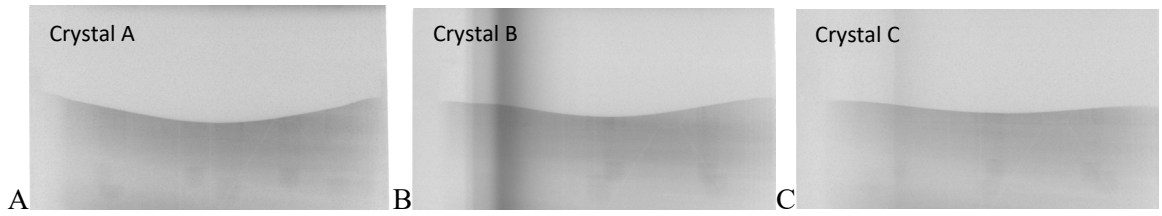

Fig. 1. 2D X-ray in-situ visualization of the PVT growth processes using the SiC sources A, B and C: Comparison of the shape of the growth interfaces of the crystals A, B, and C at about the midpoint of the growth process.

If all other properties of the SiC source material are similar, a higher packing density is generally preferred for a stable PVT process. Consistent with this somewhat general statement, the growth run using SiC source C with the largest SiC powder size distribution and the highest packing density of 1.50 g/cm^3 exhibits the most favorable, almost flat and slightly convex growth interface. Surprisingly, the crystal B of the growth run with source B and a slightly lower packing density of 1.44 g/cm^3

(compared to growth run C) exhibits a pronounced convex area in the center of the crystal. This is unexpected because growth run A with SiC source A and the lowest packing density of 1.31 g/cm^3 gain shows a flatter growth interface between growth runs B and C.

Temperature Field. The calculated temperature fields for the different process conditions of the growth runs A, B, C agree very well with the experimental conditions. The deviation of the data is in the range of 10-20°C (Table 2), which corresponds to an error of less than 1% at T>2000°C. The type of SiC powder source (B and C) does not significantly affect the temperature field at the seed (similar axial temperature gradients of about 6.3(+/-0.1)°C/cm). However, in the case of coarse powder flakes (source A), a slightly larger axial T-gradient is observed due to the higher thermal conductivity of the SiC source. To rule out the influence of the heating power, which varied up to 10% between the growth experiments, computer simulations of all growth runs A, B and C were compared at a virtual reference power of 10.25 kW (Table 3). Comparing the calculated temperature fields of the three growth runs with the same heating power (initial growth conditions at the start of the process), the temperatures at the top of the growth cell as well as at the seed surface hardly differ. However, the coarse grain source A (compared to powder sources B and C) shows a slightly higher temperature at the seed (about 10°C) and an axial temperature gradient in the gas space that is about 15% higher, which (for the given basic crucible design and overall T-field setting) corresponds to the more convex growth interface developed during the subsequent growth process (see also growth interface at 120h and previous work [3]).

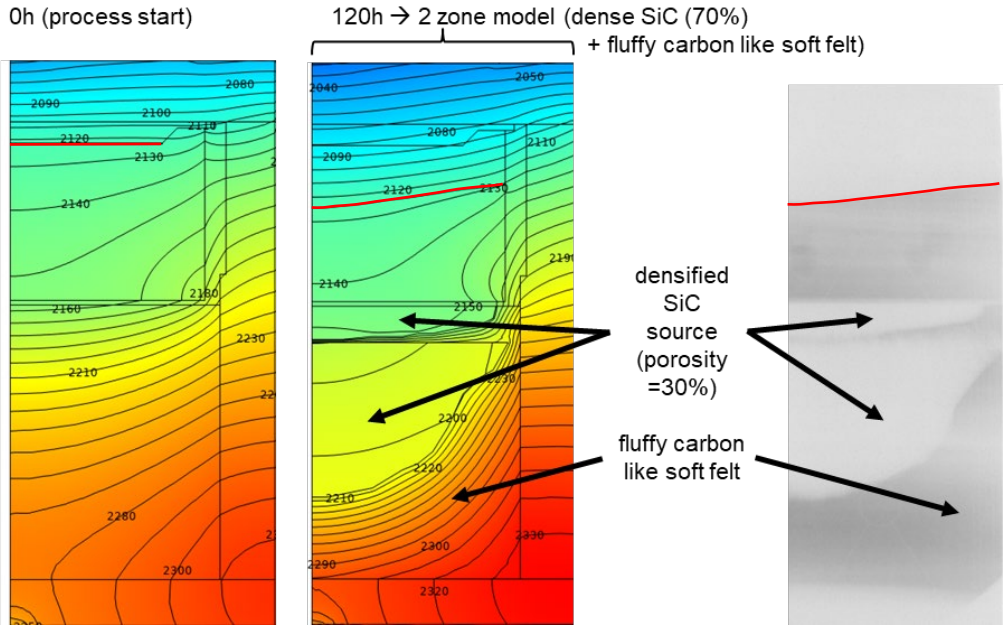

Fig. 2. Calculated temperature field of the growth cell (source C) at the beginning (0h, left) of the growth process and at the end (120h, center). The dimensions of the morphologic changes inside the source materials are deduced from the in-situ X-ray image of the growth cell (right). Crystal growth interfaces are indicated in red color.

Table 2. Comparison of experimental data and computer simulation of the temperature field at the beginning of the growth process (0h).

Number	Power (exp) [kW]	$T_{crucible}$ (exp) [°C]	$T_{crucible}$ (sim) [°C]	T_{seed} (sim) [°C]	$T_{gradient}$ (sim) [°C/cm]
Source A	10.25	2030	2035	2114	7.4
Source B	11	2095	2085	2166	6.3
Source C	10.5	2040	2048	2126	6.5
FAU ref.	10.25		2026	2101	6.4

Table 3. Normalized comparison of the calculated T-field at the reference heating power of 10.25 kW (0h).

Number	Power (exp) [kW]	$T_{crucible}$ (exp) [°C]	$T_{crucible}$ (sim) [°C]	T_{seed} (sim) [°C]	$T_{gradient}$ (sim) [°C/cm]
Source A	10.25	2030	2035	2114	7.4
Source B	10.25		2026	2101	6.4
Source C	10.25		2028	2104	6.6
FAU ref.	10.25		2026	2101	6.4

Altogether, the chosen hot zone design is quite insensitive to the applied SiC source material (type of powder or coarse grain flakes).

Evolution of the SiC crystal and source. Fig. 3 shows the evolution of the SiC crystals and sources for all three growth runs A, B and C at an advanced process stage of 120h, 91h and 120h, respectively, exhibiting a comparable value of SiC source consumption. The changes in crystal shape and source morphology were used in the computer simulation of the temperature field in Fig. 2. The source material was treated using a two-zone model, which has densified SiC feed regions (assumed to be 70% of the SiC bulk density) and a fluffy carbon skeleton with physical properties similar to a soft carbon felt insulation [6]. The development of this outer carbon boundary acts as an expanding thermal insulator during the growth process and causes the temperature at the top of the crucible to drop steadily by about 30-40°C (Tables 2 and 4). Nevertheless, the temperature at the growth interface remains quite stable throughout the process, varying only 5-10°C (Tables 2 and 4). However, during the transition of the starting material (=expansion of the fluffy carbon zone), the thermal properties in the upper densified disc-like structure change. The latter changes the T-gradient in the gas space (Tables 2 and 4) as well as the sublimation properties at the top of the SiC source material. In the case of source C, the T-gradient drops from 6.5 to a low value of 4.9°C/cm. However, in the case of source B, the T-gradient remains almost the same (6.3→5.9°C/cm). In previous studies, an increased axial temperature was found due to (i) an initial different specification compared to the standard SiC powder or (ii) a material transformation of a SiC source during the growth process [3].

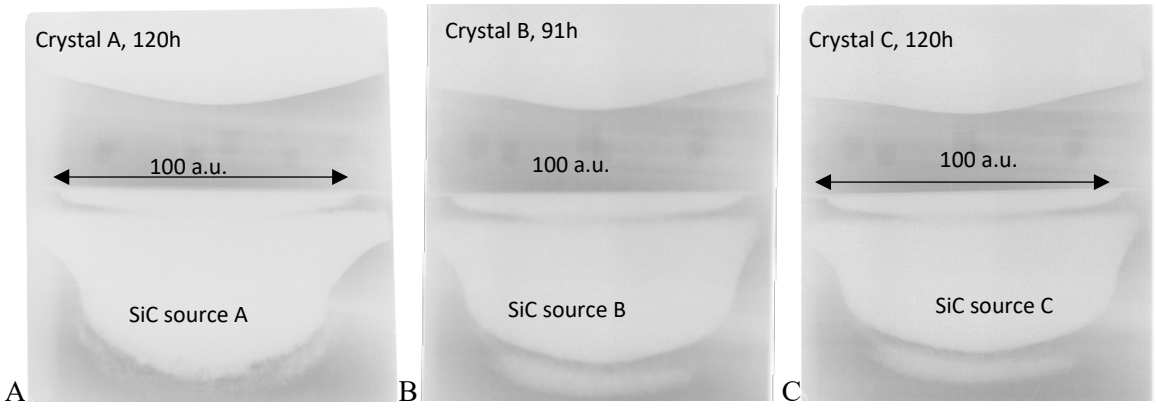

Fig. 3. 2D X-ray in-situ visualization of the PVT growth processes using the SiC sources A, B and C: Comparison of the shape of the growth interfaces of the crystals A, B, and C as well as the morphologic changes of the SiC sources at an advanced process stage of 120h, 91h and 120h (= comparable value of SiC source consumption).

Noteworthy, source A, which developed a significantly higher axial T-gradient between source and growth interface at the beginning of the growth process (7.4°C/cm compared to 6.4 and 6.6°C/cm for sources B and, respectively) during the growth process, is responsible for the evolution of a more convex growth interface (compared to sources B and C).

Table 4. Comparison of experimental data and computer simulation of the temperature field at the end of the growth process (120h).

Number	Power [kW]	$T_{crucible}$ (sim) [°C]	$T_{crystal}$ (sim) [°C]	$T_{gradient}$ (sim) [°C/cm]
Source A	10.25	1998	2106	5.7
Source B	11	2047	2171	5.9
Source C	10.5	2019	2127	4.9

Mass Transport Calculation. The performed mass transport calculations suggest that the effective surface area per source volume has an impact on the results. Here the results under the assumption that the source region under powder evolution reduces the initial area per volume ratio, but still shows a correlation of the one of the virgin powder, are reported. Due to the different growth rates the snapshot in time at 120h, 91, and 120h is shown for source A, B and C respectively. At this moments in time the crystals in the middle have roughly the same thickness (~20mm). In Fig. 4 a), b) and c) the SiC_2 partial pressure results for sources with an effective surface to area ratio of 24, 80 and 171 m^2/m^3 are shown. It is visible that the crystal with the coarse powder Source A is exposed to a significantly higher SiC_2 partial pressure in the middle. This is not fully reflected in the growth rate (see Fig 4. d) and e)), because this middle region is also positioned at a region with higher temperature compared to the crystal edge, and therefore also shows higher equilibrium partial pressure. The same is true to a lower extend for Source B. In contrast, Source C is exposed to the flattest SiC_2 partial pressure distribution and also shows the flattest growth rate in agreement with the slightly flatter crystal shape. It should be remarked that the higher growth rates for source B, given by the higher overall temperature, can be expected to have some influence on the sublimation kinetics and potentially could explain the minor difference in the otherwise similar growth behavior for Source B and C.

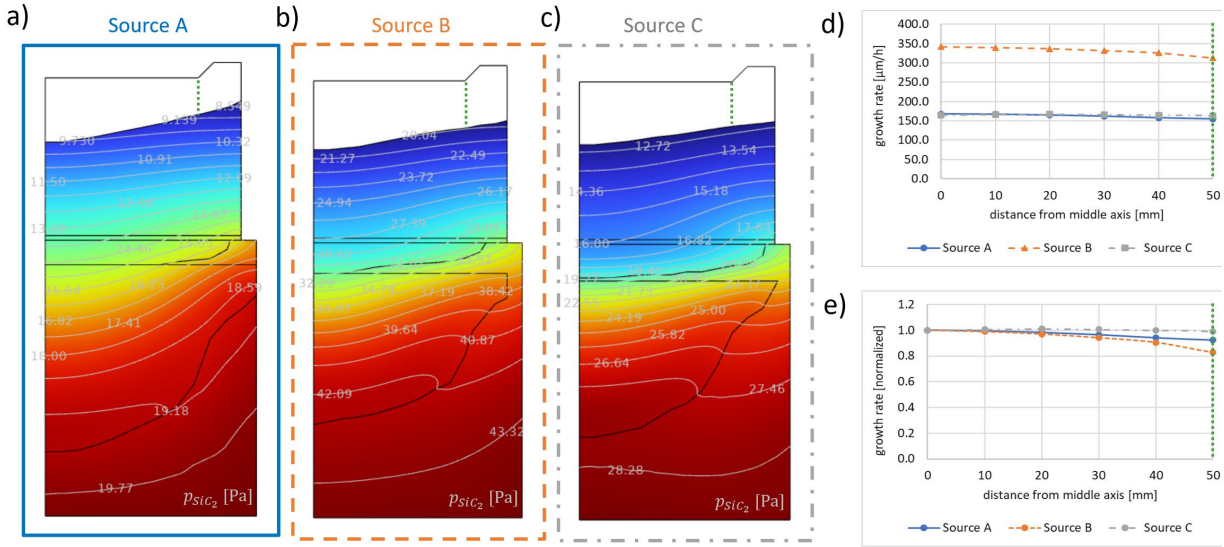

Fig. 4. Computed partial pressure a) to c), growth rate d) and normalized growth rate e) for the effective surface to volume ratio of 24, 80 and 171 m^2/m^3 for Source A (@120h), B(@91h) and C(@120h).

The usage of a minimal mass transport model should be considered as a first attempt to understand the differences, observed with different powders, qualitatively. The current model includes crude simplifications, e.g. densified powder region is treated with uniform parameters. In reality, at least the upper and lower densified region are expected to have quite different properties. Some model parameters like the surface to volume ratio should be determined and even more model parameters can be reasonably introduced if support by experimental data is provided (e.g. powder density and morphology dependent diffusion coefficients). To reduce the experimental effort in the future accurate powder evolution models would be called for. Although some studies have addressed the description of the SiC powder evolution during PVT growth, the ongoing processes during

sublimation and recrystallization inside the source material are quite complex and for example the assumption of evolving round particles is insufficient [10]. One would have to consider the morphology of the initial SiC source particle size and shape distribution, which then evolves into highly condensed and partially needle-like structures [4, 6, 11, 12]. To date, no such attempt to develop a general model has been successful.

Looking at the dimension of the condensed SiC disk on top of the SiC sources A, B and C at the end of growth (120h), we observed a smaller lateral dimension in the case of growth run B (85a.u. compared to 100a.u. for A and C, no image shown here). In this case of crystal B, the final sublimation area at the top of the SiC source was significantly smaller, resulting in a slight concentration of SiC mass transport in the central region of the growth cell. In the past, this type of concentrated mass transport behavior (typically in the final growth process period) has also been observed in several growth runs using SiC source materials prepared in our own laboratory (results not shown here).

The slightly different effect of the evolution of the almost equal SiC sources B and C on the PVT growth process (= crystal B exhibits a slightly more convex growth interface than crystal C) indicates that a careful selection of the SiC powder size distribution is mandatory for a reproducible PVT growth process with a high crystal yield.

Conclusions

Although all three SiC source materials led to almost similar thermal boundary conditions in the initial growth stage, the axial temperature gradient inside the gas room is higher in case of the coarse grain source A compared to the sources B and C. This observation was attributed as main reason for the more convex shape of crystal A (compared to the crystals B and C). The further evolution of the three sources depended significantly on the initial size and shape distribution. The theoretical treatment of the mass transport from the source to the growing crystal using an effective surface area per source volume supports the observed crystal shape evolution very well. A strong influence on the growth process is developed by the rate and degree of densification of the SiC source material and the formation of needle-like structures. The formation of a residual fluffy carbon skeleton acts as thermal insulator. In-situ X-ray visualization is a powerful tool to follow the evolution of the SiC source and crystal. Until now, it has not been possible to accurately predict the effect of the evolving SiC powder source on the mass transport in the system, which determines the evolving crystal shape. The present results clearly show that a high yield in SiC boules production requires a careful supply chain of SiC source material with reproducible properties.

References

[1] P.J. Wellmann, *Semicond. Sci. Technol.,* 33, 103001 (21pp) (2018)

[2] O. M. Ellefsen, M. Arzig, J. Steiner, P. Wellmann,P. Runde, *Materials,* 12, 19, 3272 (2019)

[3] M. Arzig, M. Salamon, N. Uhlmann, B. A. Johansen,P. J. Wellmann, *Materials Science Forum,* 924, 245 (2018)

[4] P.J. Wellmann *et al.*, *Journal of Crystal Growth,* 216, 263 (2000)

[5] J. Steiner, M. Arzig, A. Denisov,P. J. Wellmann, *Crystal Research and Technology,* 55, 2, 1900121 (2020)

[6] M. Arzig, J. Steiner, M. Salamon, N. Uhlmann,P. J. Wellmann, *Materials,* 12, 16, 2591 (2019)

[7] M. Pons *et al.*, *Mater.Sci.Eng.B,* 61-63, 18 (1999)

[8] M. Selder *et al.*, *Journal of Crystal Growth,* 211, 333 (2000)

[9] R. Ma, H. Zhang, V. Prasad,M. Dudley, *Crystal Growth & Design,* 2, 3, 213 (2002)

[10] P.J. Wellmann *et al.*, *Mat.Sci.Forum,* 457-460, 55 (2004)

[11] P. Wellmann *et al.*, *Journal of Crystal Growth,* 275, 1-2, e1807 (2005)

[12] P. J. Wellmann, D. Hofmann, L. Kadinski, M. Selder, T. L. Straubinger,A. Winnacker, *Journal of Crystal Growth,* 225, 312 (2001)